The Journal of the Korean Society of Oceanography
Vol. 29, No. 2, pp. 95-106, June 1994

# Three-Dimensional Numerical Model Experiments of Tidal and Wind-Driven Currents in Chinhae Bay

CHA-KYUM KIM
*Division of Environment, National Fisheries Research and Development Agency, Yangsan-gun, Kyungsangnam-do 626-900, Korea*

# 진해만 조류 및 취송류의 3차원 수치모형실험

김 차 겸
국립수산진흥원 환경과

Tidal and wind-driven currents in Chinhae Bay are investigated using a three-dimensional numerical model developed by Kim et al. (1993). The simulations indicate that the flow patterns in the bay are predominated by the bathymetry, wind and river inflow, and the effects of wind on the flow pattern in the inner bay are much stronger than those in the entrance channel. Computed tidal currents coincide with the field measurements. The horizontal and vertical velocities of tidal and residual currents are strong in the entrance channel of the bay, whereas the velocities are relatively weak in the western and northern parts of the bay. Computed velocity fields show the expected phase difference between the velocities in the surface and those in the bottom layer, and these characteristics are more remarkable during the spring tide than the neap tide. The surface currents in the bay depend strongly on the wind and river inflow, and such phenomena are more remarkable during the neap tide than the spring tide.

김 등(1993)에 의해 개발된 3차원 해수유동 수치모델을 사용하여 진해만의 조류 및 취송류를 해석하였다. 만내의 흐름은 주로 지형, 바람 및 하천유출수에 의해 지배되며, 만 입구의 수로보다 내만에서 바람의 영향을 더 강하게 받는다. 계산된 조류는 현장관측과 잘 일치한다. 조류 및 조석잔차류의 수평 및 연직 유속은 만 입구의 수로에서는 강하나, 진해만의 서부해역과 북부해역에서는 상대적으로 약하게 일어났다. 저층과 표층 사이에 유속의 위상차가 일어나며, 위상차는 소조기보다 대조기에 더 뚜렷하게 나타났다. 또한, 만내에서 표층흐름은 바람 및 하천유출류에 의해 강하게 지배되며, 이러한 현상은 대조기보다 소조기에 더 뚜렷하게 나타났다.

## INTRODUCTION

Chinhae Bay, located in the southeastern sea of Korea, is a semi-enclosed bay with complex topography and geometry (Fig. 1). The maximum and average depths of the bay reach about 45 m and 15 m, respectively. The water exchange of the bay takes place through Kaduk and Kyunnaeryang channels, and 86~90 % of the exchange occurs through Kaduk channel (Kim, 1984).

Red tides in Chinhae Bay occur every year since the 1980's (NFRDA, 1989), and oxygen deficiency occurs in the bottom layer of the western and northern parts of the bay in summer since the 1980's (Hong, 1987; NFRDA, 1989; Lee et al., 1993). This strong oxygen depletion harms marine organisms and causes great damage to fisheries, and therefore the productivity of the bay has declined significantly. To conserve and control the fish- and culture-farm of the bay, the polluted water and sediment

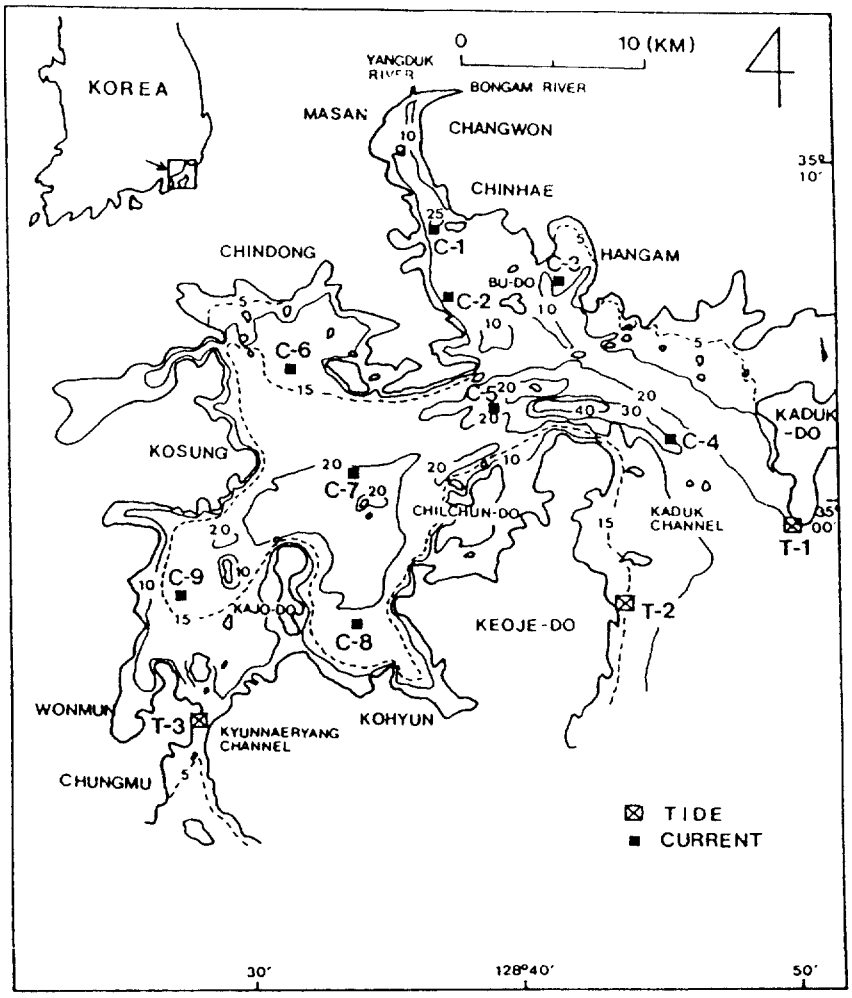


Fig. 1. Bottom topography of Chinhae Bay.

must be improved. To establish a sound coastal management plan to improve fish- and culture-farm environments, a thorough understanding of the 3-D water circulation is required. Circulation and transport associated with the tidal propagation constitute one of the most important and everlasting driving mechanism in coastal waters. The non-linear term in the coastal zone is predominant, and the non-linear mechanism generates net circulation over the shallow water in addition to the tidal excursion. This net residual transport is usually responsible for carrying constituents to areas much beyond the extent of tidal excursion over the time span of weeks or months. The tidal residual circulation pattern is extremely difficult to establish by measurement as only a limited number of current meters can be employed. Numerical model has been become one of the important planning tools widely used among coastal engineers in the past two decades. To date, there exist a large number of models which are formulated for various purposes, and solved by different numerical techniques (Leendertse and Liu, 1975; Horiguchi et al., 1977; Sheng, 1983; Oey, 1988; Blumberg and Herring, 1987; Kim, 1992). The residual circulation of a coastal area should be studied by considering both barotropic and baroclinic modes. Because the surface currents in Chinhae Bay is

strongly influenced by wind and river inflow (Kim et al., 1994), the influence of wind and river inflow on the flow pattern of the bay should be studied. Therefore, 3-D model of the wind- and river inflow-driven currents is required, because the currents cannot be described well by 2-D simulations (Kim et al., 1994). 3-D hydrodynamic model employed in the present study is BACHOM-3 developed by Kim et al. (1993). The model BACHOM-3 includes tides, wind, freshwater inflows, density effects and the effect of the Earth's rotation. This model provides a basic framework for future study on the occurrence mechanism of eutrophication and oxygen deficient water masses in Chinhae Bay.

## GOVERNING EQUATIONS

Assuming the hydrostatic pressure distribution and the Boussinesq approximation, the governing equations for an incompressible fluid in a three-dimensional (x, y, z) coordinate system with the z-axis vertically upwards are:

$$\frac{\partial u}{\partial x}+\frac{\partial v}{\partial y}+\frac{\partial w}{\partial z}=0 \tag{1}$$

$$\frac{\partial u}{\partial t}+u\frac{\partial u}{\partial x}+v\frac{\partial u}{\partial y}+w\frac{\partial u}{\partial z} =fv-\frac{1}{\rho_o}\frac{\partial p}{\partial x}+\frac{\partial}{\partial x}\left(\varepsilon_x\frac{\partial u}{\partial x}\right)+ +\frac{\partial}{\partial y}\left(\varepsilon_y\frac{\partial u}{\partial y}\right)+\frac{\partial}{\partial z}\left(\varepsilon_z\frac{\partial u}{\partial z}\right) \tag{2}$$

$$\frac{\partial v}{\partial t}+u\frac{\partial v}{\partial x}+v\frac{\partial v}{\partial y}+w\frac{\partial v}{\partial z} =-fu-\frac{1}{\rho_o}\frac{\partial p}{\partial y}+\frac{\partial}{\partial x}\left(\varepsilon_x\frac{\partial v}{\partial x}\right)+ +\frac{\partial}{\partial y}\left(\varepsilon_y\frac{\partial v}{\partial y}\right)+\frac{\partial}{\partial z}\left(\varepsilon_z\frac{\partial v}{\partial z}\right) \tag{3}$$

$$\frac{\partial p}{\partial z}=-\rho g \tag{4}$$

where u, v and w are the velocities in x, y and z directions respectively, p is the pressure, $\rho_o$ is the reference density, f is the Coriolis parameter as $2\omega\sin\phi$ where $\phi$ is the latitude, $\omega$ is the angular speed of earth rotation, t is the time, g is the gravity, $\rho$ is the density, and $\varepsilon_x$, $\varepsilon_y$ and $\varepsilon_z$ are the eddy viscosity coefficients in x, y and z directions, respectively.

After substituting Eq. (4) to Eqs. (2) and (3), and taking the vertical integration of Eqs. (1) to (3) for the kth layer, and also using a streamline condition at the surface and the bottom, the governing equations become:

$$\frac{\partial \zeta}{\partial t}+\sum_{k=1}^{b}\left\{\frac{\partial (uh)_k}{\partial x}+\frac{\partial (vh)_k}{\partial y}\right\}=0,\ k=1,2,\cdots,b \tag{5}$$

$$\frac{\partial u}{\partial t}+u\frac{\partial u}{\partial x}+v\frac{\partial u}{\partial y}+w\frac{\{(u)_{k-1/2}-(u)_{k+1/2}\}}{h} =fv-g\frac{\rho_\zeta}{\rho_o}\frac{\partial \zeta}{\partial x}-\frac{g}{\rho_o}\int_\zeta^z\frac{\partial \rho}{\partial x}dz +\frac{\partial}{\partial x}\left(\varepsilon_x\frac{\partial u}{\partial x}\right)+\frac{\partial}{\partial y}\left(\varepsilon_y\frac{\partial u}{\partial y}\right) +\left\{\left(\varepsilon_z\frac{\partial u}{\partial z}\right)_{k-1/2}-\left(\varepsilon_z\frac{\partial u}{\partial z}\right)_{k+1/2}\right\}/h \tag{6}$$

$$\frac{\partial v}{\partial t}+u\frac{\partial v}{\partial x}+v\frac{\partial v}{\partial y}+w\frac{\{(v)_{k-1/2}-(v)_{k+1/2}\}}{h} =-fu-g\frac{\rho_\zeta}{\rho_o}\frac{\partial \zeta}{\partial y}-\frac{g}{\rho_o}\int_\zeta^z\frac{\partial \rho}{\partial y}dz +\frac{\partial}{\partial x}\left(\varepsilon_x\frac{\partial v}{\partial x}\right)+\frac{\partial}{\partial y}\left(\varepsilon_y\frac{\partial v}{\partial y}\right) +\left\{\left(\varepsilon_z\frac{\partial v}{\partial z}\right)_{k-1/2}-\left(\varepsilon_z\frac{\partial v}{\partial z}\right)_{k+1/2}\right\}/h \tag{7}$$

where $\zeta$ is the displacement of the free surface, b represents the bottom layers, h is the layer thickness and $\rho_\zeta$ is the density at the surface. Vertical velocity at the interface between layer k and k+1 can be estimated as:

$$w_{k+1/2}=-\sum_{l=k}^{b}\left\{\frac{\partial (uh)_l}{\partial x}+\frac{\partial (vh)_l}{\partial y}\right\} \tag{8}$$

Salinity distribitions are obtained by solving 3-D advection-diffusion equation of salinity. A linear equation of state on density is assumed by Yanagi et al. (1986):

$$\rho=\rho_f(1+0.000757\,S) \tag{9}$$

where $\rho$ is the water density, $\rho_f$ is the density of

freshwater (=0.999), and S is the salinity.

## BOUNDARY CONDITIONS

The shear stress at the surface is given as:

$$\tau_s=\rho_a\gamma_s^2 W|W| \tag{10}$$

where W is the wind velocity (m/s), $\rho_a$ is the air density (=0.00123 g/cm$^3$), $\gamma_s^2$ is the drag coefficient of air which is given by Large and Pond (1981):

$$\gamma_s^2=\begin{cases}1.2\times10^{-3}, & W<11\ \text{m/s}\\ (0.49+0.0065\,W)\times10^{-3}, & 11\le W<25\ \text{m/s}\end{cases} \tag{11}$$

A partial-slip condition is imposed at the sea bed by assuming that shear stress is a quadratic function of the bed velocity, and the no-flux condition through the bottom is applied. Introducing a bottom friction coefficient, the imposed relation can be written in the following form:

$$\left(\varepsilon_z\frac{\partial u}{\partial z}\right)_b=\gamma_b^2 u\sqrt{u^2+v^2}$$
$$\left(\varepsilon_z\frac{\partial v}{\partial z}\right)_b=\gamma_b^2 v\sqrt{u^2+v^2} \tag{12}$$

where $\gamma_b^2$ is the bottom friction coefficient.

The vertical eddy viscosity is given as:

$$\varepsilon_z=\gamma_i^2\Delta z^2\sqrt{\left(\frac{\partial u}{\partial z}\right)^2+\left(\frac{\partial v}{\partial z}\right)^2} \tag{13}$$

where $\gamma_i^2$ is the internal friction coefficient, and $\Delta z$ is the vertical grid size.

At the closed boundary no-flux and full-slip conditions are applied, and at the seaward boundary water levels are prescribed. The Bongam River and Yangduk River which are located in the northern part of Chinhae Bay are modeled with discharge rates of 20 m$^3$/s, respectively. The initial velocity is taken to be zero, and the water surface is taken to be at mean sea level. Boundary forcings consist of tides, winds and fresherwater inflows.

## NUMERICAL SOLUTION

ADI (Alternating Direction Implicit) scheme is used to solve the governing equations, and upwind differencing is used to solve advection-diffusion equation. A space-staggered grid is used, and the computational process is given by Kim (1992) and Kim et al. (1993). The open boundaries are forced with $O_1$, $K_1$, $M_2$ and $S_2$ tidal constituents using the data at Kaduk and Kyunnaeryang channels listed in Table 1 (KORDI, 1983).

The model BACHOM-3 (Kim et al., 1993) is run with horizontal viscosity of 24 m$^2$/s, bottom

Table 1. Tidal harmonic constants used in the hydrodynamic model (KORDI, 1983)

| St. | Constituent | Speed (°/h) | Amplitude (cm) | Phase lag (°) |
|---|---|---|---|---|
| T-1 | $O_1$ | 13.94 | 3.69 | 126.55 |
| | $K_1$ | 15.04 | 6.12 | 169.82 |
| | $M_2$ | 28.98 | 53.83 | 243.72 |
| | $S_2$ | 30.00 | 32.41 | 291.34 |
| T-2 | $O_1$ | 13.94 | 4.10 | 125.88 |
| | $K_1$ | 15.04 | 6.35 | 168.91 |
| | $M_2$ | 28.98 | 54.37 | 244.53 |
| | $S_2$ | 30.00 | 32.40 | 291.92 |
| T-3 | $O_1$ | 13.94 | 4.63 | 130.51 |
| | $K_1$ | 15.04 | 7.52 | 176.92 |
| | $M_2$ | 28.98 | 68.16 | 253.41 |
| | $S_2$ | 30.00 | 40.22 | 302.80 |

Table 2. Computational conditions of flow field

| Parameters | Values |
|---|---|
| Horizontal grid interval | $\Delta x=\Delta y=500$ m |
| Time interval | $\Delta t=40$ sec |
| Vertical grid interval | Level 1: 4 m(0~4 m)<br>Level 2: 6 m(4~10 m)<br>Level 3: 6 m(10~16 m)<br>Level 4: below 16 m |
| Horizontal eddy viscosity coefficient | $\varepsilon_x=\varepsilon_y=24$ m$^2$/s |
| Initial salinity concentration | 33.0‰ |
| Salinity concentration at open boundary | 33.0‰ |
| Internal friction coefficient | $\gamma_i^2=0.0025$ |
| Bottom friction coefficient | $\gamma_b^2=0.0050$ |
| Coriolis parameter | $f=8.37\times10^{-5}$ |
| Wind direction | N and S |
| Wind speed | 4.14 m/s |
| Discharge of Bongam River | 20.0 m$^3$/s |
| Discharge of Yangduk River | 20.0 m$^3$/s |

friction coefficient of 0.005 and internal friction coefficient of 0.0025 throughout the bay. The computational time step is 40 sec, and the horizontal grid size is 500 m. There are 78×81 horizontal cells and 4 vertical levels. the vertical grid size varies from 4 to 29 m. The computational conditions are summarized in Table 2.

## RESULTS

### *Tidal currents*

With computational conditions summarized in Table 2, computations during the spring and neap tides are made on the numerical grid. The tides at the model's open boundary are generated using composited tidal elevation of the field measurements given in Table 1. The simulation was carried out for 49.8 hours of physical time on a 80486 personal computer. The flow patterns after 24.9 hours of the simulation were selected, because the system becomes stable at this stage. The computed current fields without wind in the levels 1 and 3 are shown in Fig. 2. The simulations indicate that the propagation of tide in the study area is dominated by the bathymetry and the geometry.

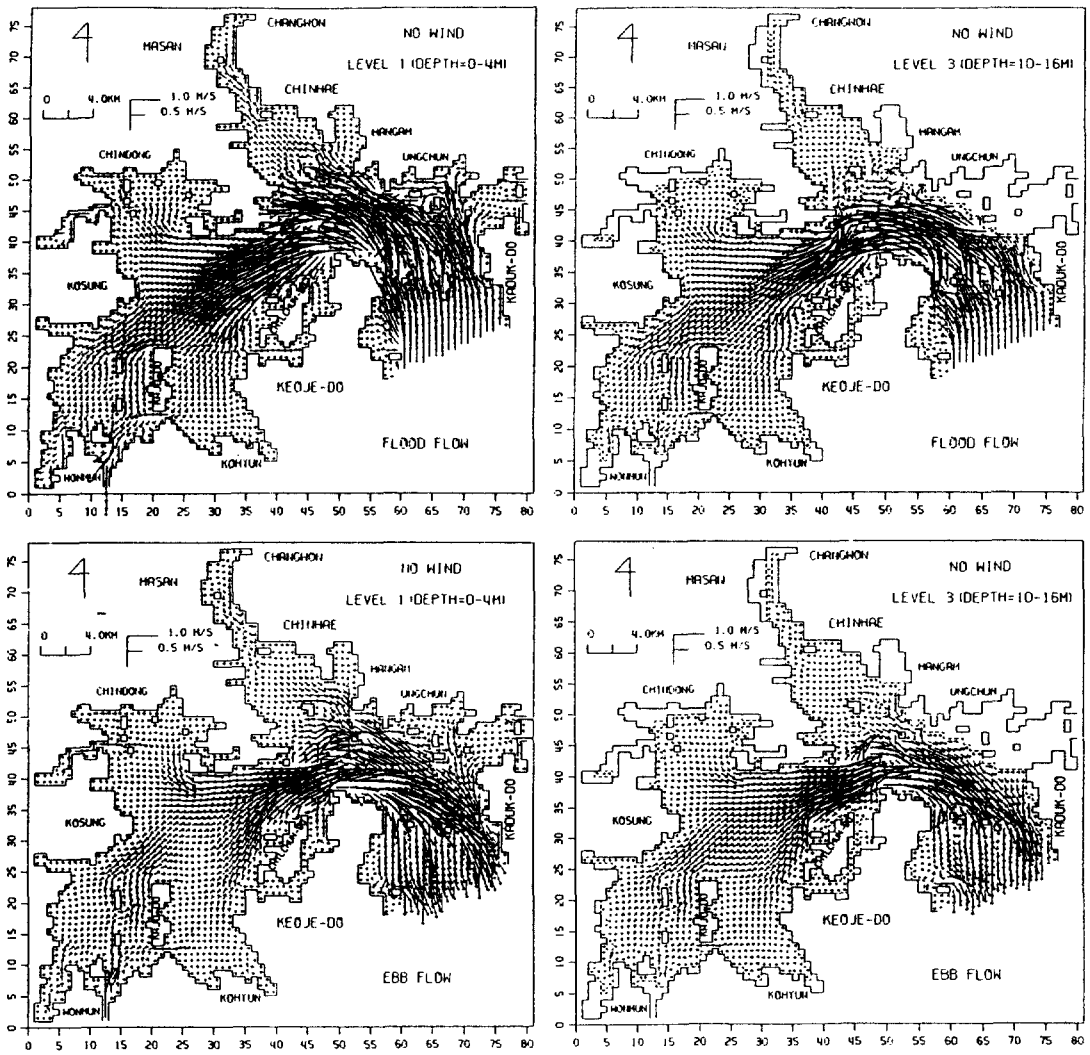


Fig. 2. Computed velocity fields without wind during the ebb and flood flows of the spring tide.

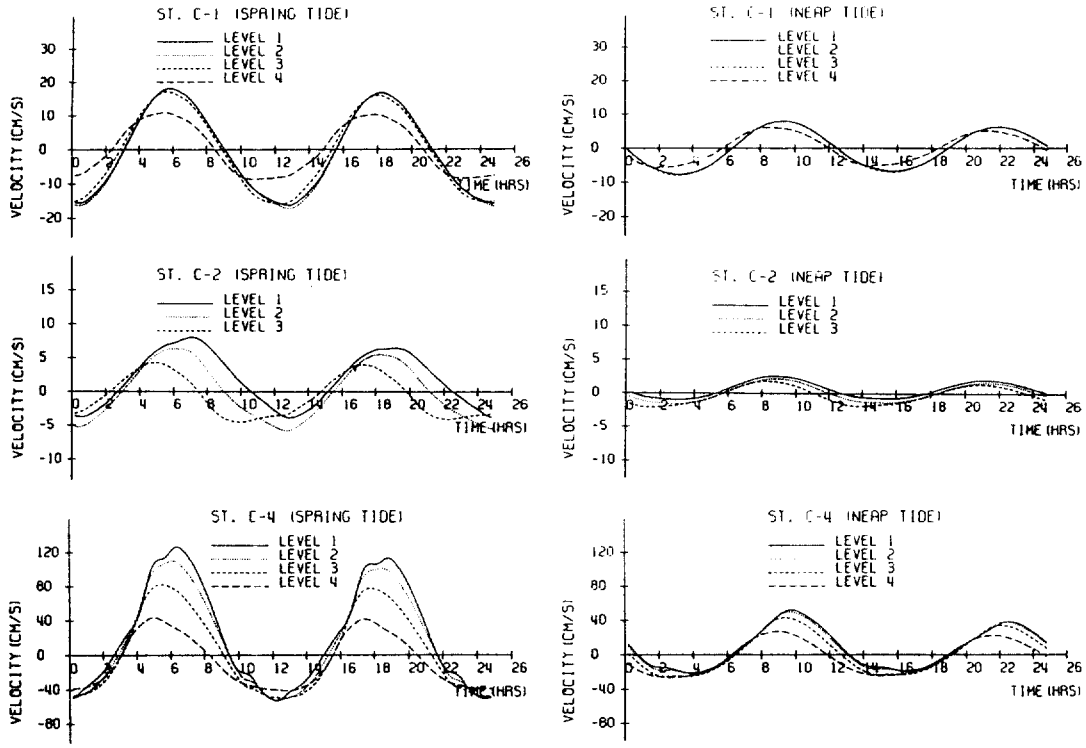


Fig. 3. North-south components of computed horizontal currents without wind during the spring and neap tides.

Due to the shallow depth and the coastal boundary , the mass fluxes in the inner part of Chinhae Bay are much weaker than those in the deeper offshore waters. The horizontal velocities in the inner bay and entrance channel of the bay are actually quite comparable in magnitude. Maximum currents in the levels 1 and 3 of Kaduk channel are 120 and 95 cm/s respectively, whereas the magnitudes of currents in the levels 1 and 3 of the western and northern parts of the bay are below about 30 and 20 cm/s, respectively. The water exchanges of the bay almost take place through Kaduk channel. The exchanges through Kyunnaeryang channel are very weak, and the influence extent is restricted to the southern part of Kajo-do.

Fig. 3 shows the north-south components of tidal velocities with time in the levels 1 to 4 of Sts. C-1, C-2 and C-4 during the spring and neap tides. We can see that the decrease in velocities with depth from the surface is considerable. The phase lag increases with the distance from the bottom, because the inertial force becomes stronger compared to the bottom friction force. These characteristics are more obvious during the spring tide than the neap tide, because the difference of the inertial and bottom friction forces during the spring tide is larger than that during the neap tide.

Comparison of the computed tidal current ellipse in the level 1 and observed one (Kim et al., 1994) in the surface layer is shown in Fig. 4, and the computed results coincide with the observed data except residual current. In both cases, the diurnal tide becomes weak, while the semi-diurnal tide becomes much more apparent. The diurnal tide in the field is larger than that in the model because of the wind effects, etc., but composited velocity amplitude of the observed diurnal and semi-diurnal tides is almost equal to the computed one.

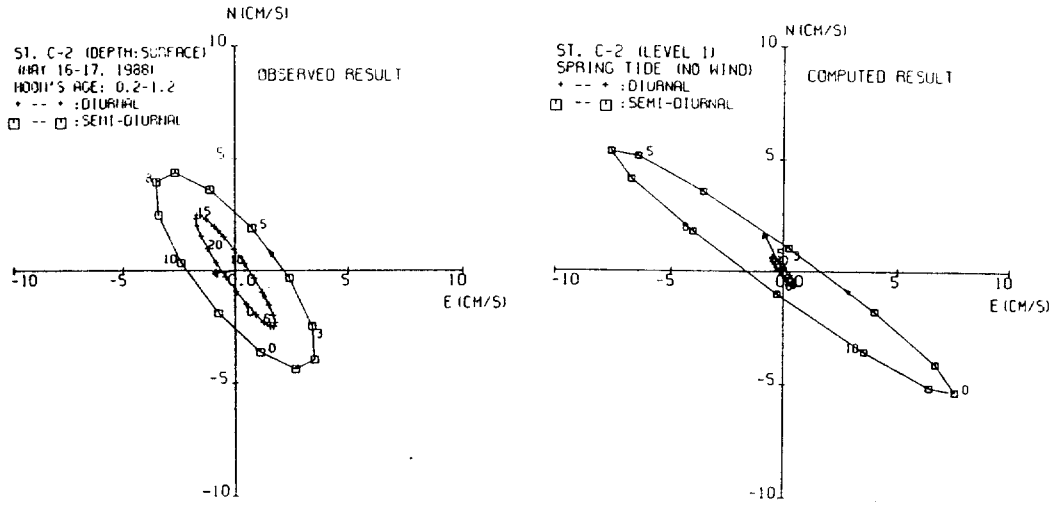


Fig. 4. Comparison of computed and observed tidal current ellipses during the spring tide.

*Wind- and river inflow-driven currents*

The patterns of wind- and river inflow-driven currents which are typically three-dimensional and complex are very difficult to understand from in situ measurements. Therefore, the numerical model would be a useful and economic tool to study such phenomena, even if its indications are not very accurate. In principle, calculations should take into account the response of the entire surrounding sea to wind forcing and large scale atmospheric pressure gradients. However, some interesting qualitative information on the response of the bay to wind forcing can be obtained from local simulations. Therefore, simulations of the direct action of the wind on the bay have been performed. The mean wind speed, 2.3 m/s, observed in Masan Meteorological Station for 6 years (1985~1990) is taken to simulate the wind-driven currents. North (N)- and south (S)-wind are used as the representative directions during winter and summer, respectively. However, because the wind speed at sea is generally 1.5~2.0 times higher than the wind measured on land (Yanagi, 1980), the wind speed input used in these simulations is 1.8 times of land-based measured value. Therefore, the simulations for uniform wind fields of 4.14 m/sec were performed during 49.8 hours. Fig. 5 shows the stick diagrams of computed horizontal velocities in the levels 1 and 3 of Sts. C-2, C-4 and C-9 without and with wind during the spring tide. The currents in the entrance channel (St. C-4) having strong currents are not greatly influenced by the wind, whereas the currents in the inner part (Sts. C-2 and C-9) of Chinhae Bay are strongly influenced by the wind. We can see that wind-driven velocity is an essential factor of the long-term water motion in the bay, because the influence of wind is very strong throughout the bay.

Fig. 6 shows the influences of the tide, wind and river inflow on the surface flow of Sts. C-1, C-2 and C-4 during the spring and neap tides. The surface currents in the bay depend strongly on the wind, and such a phenomenon is more remarkable during the neap tide than the spring tide. The effects of wind on the flow pattern in the inner bay are much stronger than those in the entrance channel. When the discharge of 20 $m^3/s$ from the Bongam River and Yangduk River inflows to Chinhae Bay, the influence of freshwater at St. C-1 is apparent. On the contrary, there is virtually no evidence of freshwater influence at St. C-2. And also, the influence of the river inflow at St. C-1 is more remarkable during the neap tide than the spring tide.

Fig. 7. shows computed vertical velocities in Sts.

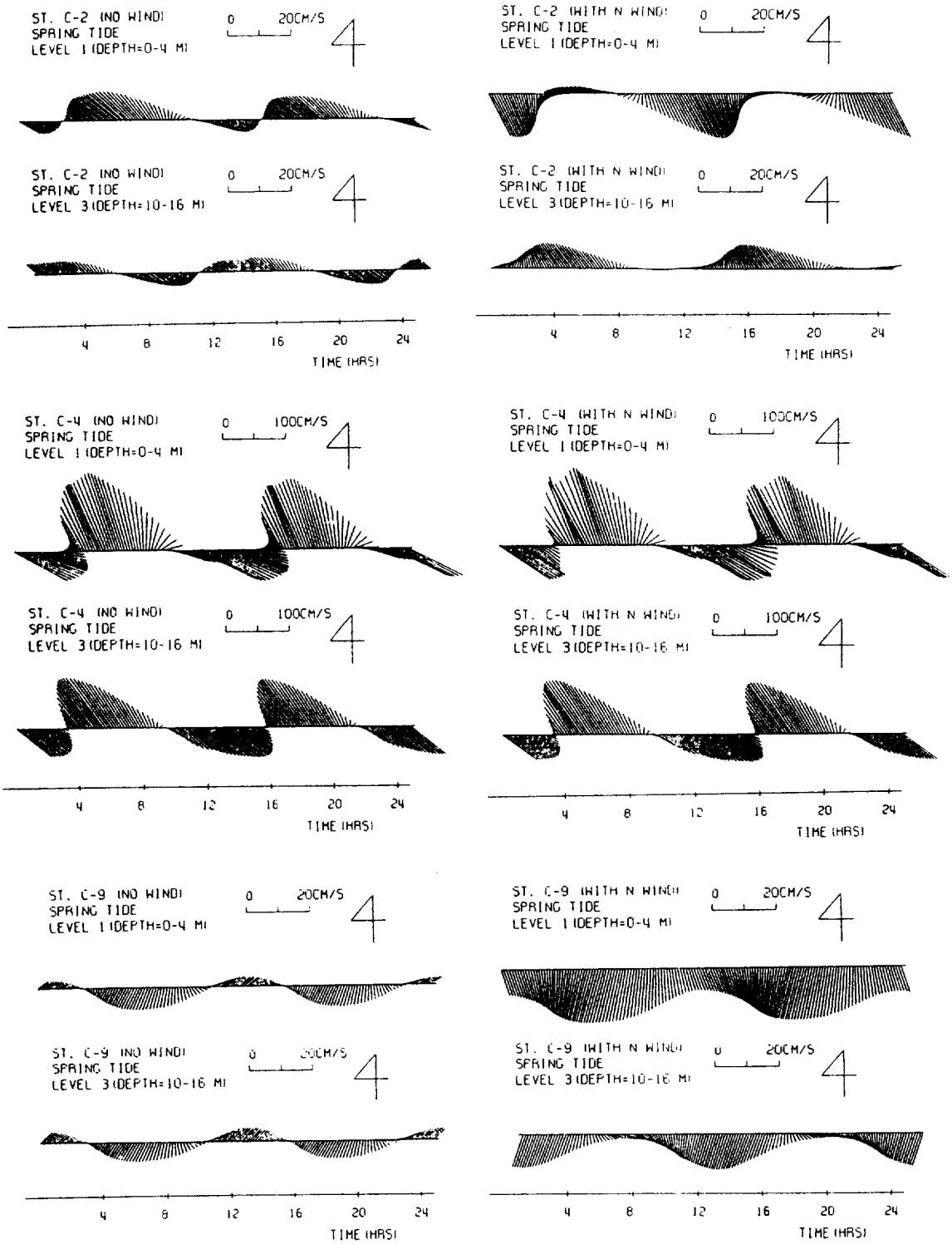


Fig. 5. Stick diagrams of computed velocities without and with wind during the spring tide.

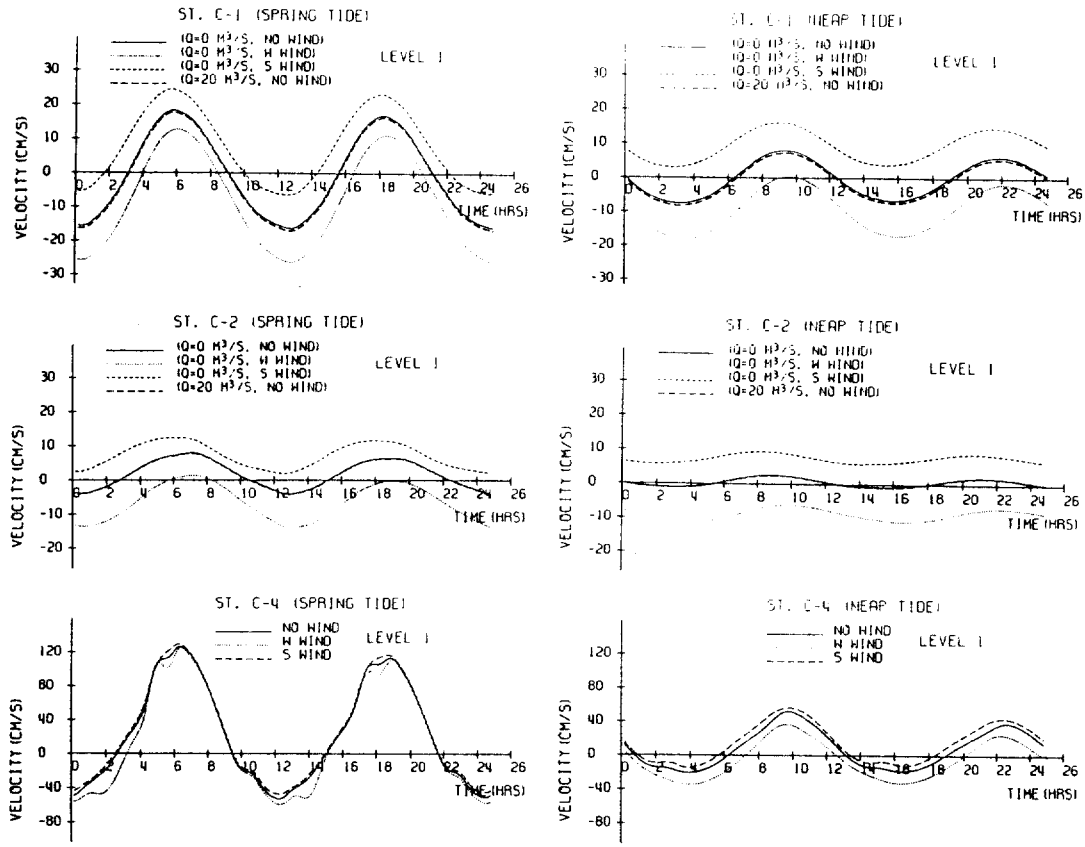


Fig. 6. North-south components of computed horizontal velocities during the spring and neap tides.

C-2, C-4, C-6 and C-9 without and with wind during the spring tide. The vertical velocities are strongly influenced by the wind, and the velocities decrease with depth from the surface. The vertical velocities in the entrance channel (St. C-4) are below 2 mm/s, whereas the velocities in the western (Sts. C-6 and C-9) and northern parts (St. C-2) of Chinhae Bay are below 0.2 mm/s. Therefore, we can see that the vertical circulations in the entrance channel are strong while the circulations in the inner bay are very weak. Consequently, oxygen deficiency in the bottom layer of the western and northern parts of the bay is presumably attributed to the weak vertical and horizontal circulations there.

Fig. 8 shows the computed residual currents in the levels 1 and 3 without and with wind during the spring tide. Computed maximum tidal residual currents (top of Fig. 8) in the levels 1 and 3 of Kaduk channel and the central channel of the bay during the spring tide are about 30 and 22 cm/s respectively, and numerous eddies take place. Tidal residual currents in the levels 1 and 3 of the western and northern parts of the bay are below 7 and 3 cm/s, respectively. Tidal residual currents in the northern part of Kajo-do go toward the north, whereas the currents in the southern part move down the bay, and the currents around Bu-do are rotating clockwise. When N- and S-winds are blowing, the residual flows in the level 1 of the inner bay correspond with the wind direction, but the residual flows in the level 3 of the inner bay go in the opposite direction. In the case of N-wind, downwelling occurs in the southern part of the bay, whereas upwelling takes place in the northern part of the bay, and the case of S-

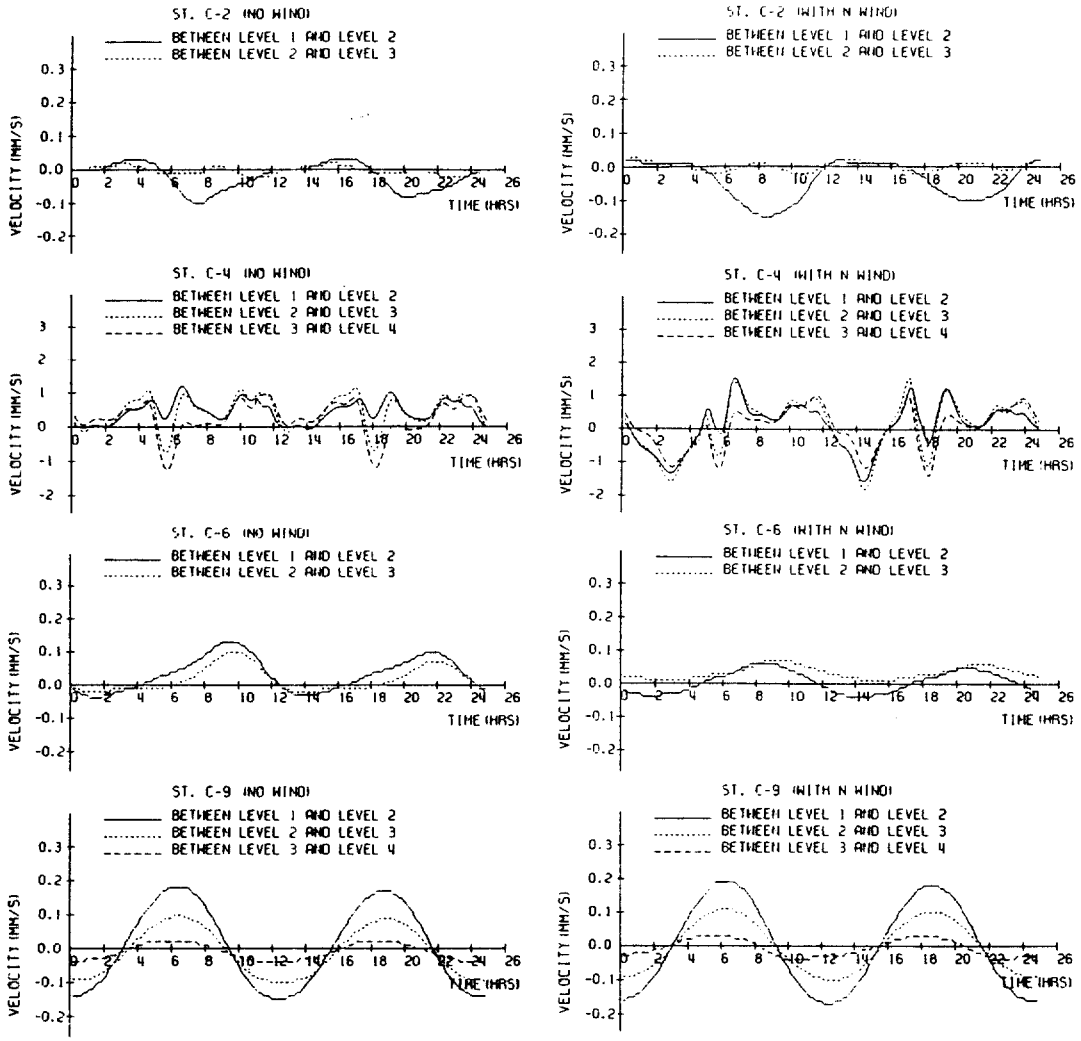


Fig. 7. Computed vertical velocities without and with wind during the spring tide.

wind is in the opposite way of N-wind. This is a well-known feature of wind-driven currents in littoral zones and lakes. The effects of wind on the residual flow pattern in the inner bay are also stronger than those in the entrance channel.

## SUMMARY AND CONCLUSIONS

Three-dimensional numerical model experiments of tidal and wind-driven currents are performed in Chinhae Bay during the spring and neap tides. The hydrodynamic model, BACHOM-3, developed by Kim et al. (1993) using an ADI finite difference scheme is employed to solve three-dimensional momentum and mass equations. The simulations indicate that the flow patterns in the bay are predominated by the bathymetry, wind and river inflow, and the effects of wind on the flow pattern in the inner bay are much stronger than those in the entrance channel. Computed tidal currents coincide with the field measurements. Strong tidal residual currrents having numerous eddies occur in Kaduk channel and the central channel of the bay, and the currents around Budo are rotating clockwise. Computed velocity fields show the expected phase difference between the

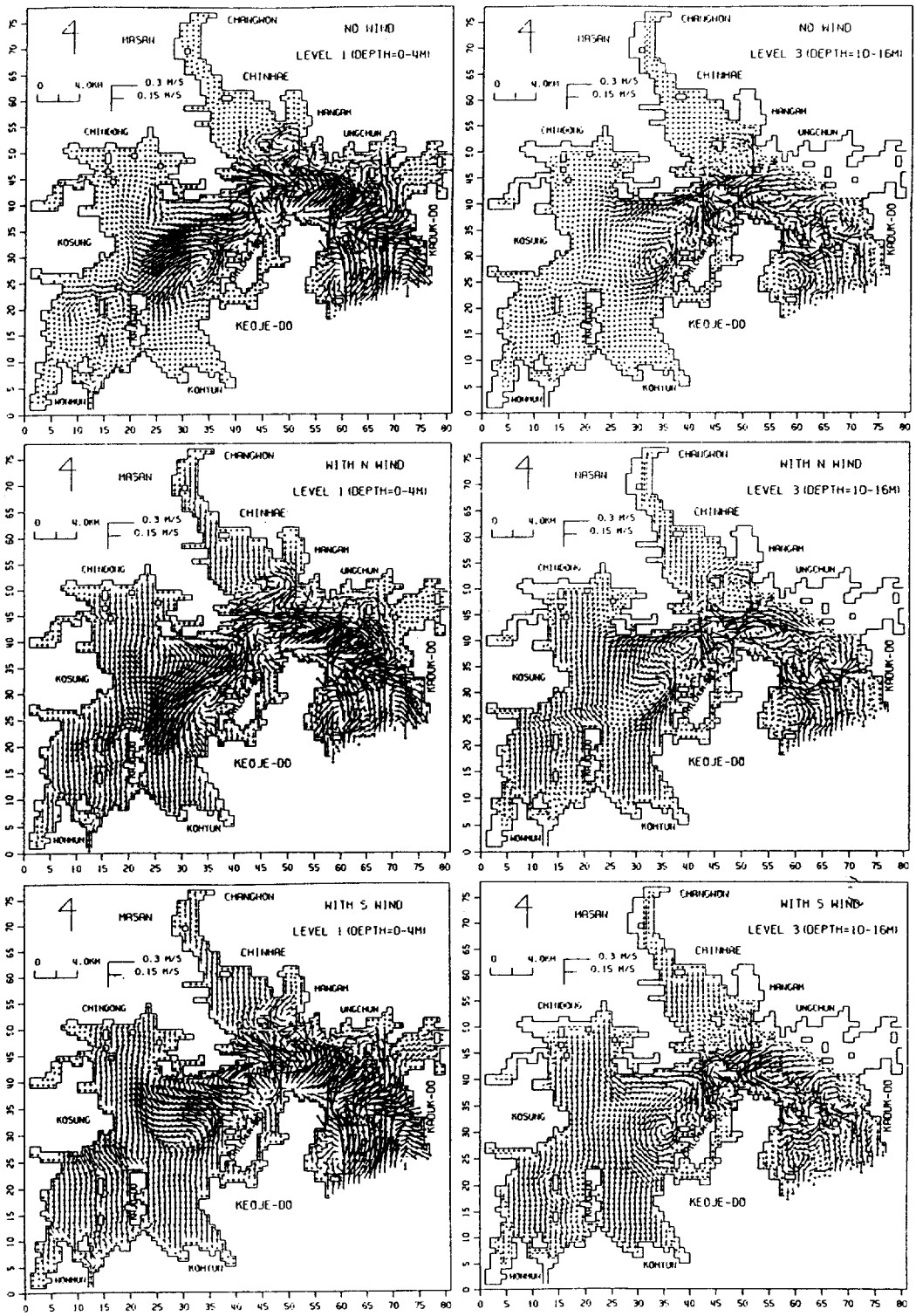


Fig. 8. Computed residual currents in levels 1 and 3 without and with wind during the spring tide.

velocities in the surface and those in the bottom layer, and these characteristics are more remarkable during the spring tide than the neap tide. The surface currents in the bay depend strongly on the wind and river inflow, and such phenomena are more remarkable during the neap tide than the spring tide. In the case of N-wind, downwelling occurs in the southern part of the bay, whereas upwelling takes place in the northern part of the bay, and the case of S-wind is in the opposite way of N-wind. Oxygen deficiency in the bottom layer of the western and northern parts of the bay is presumably attributed to the weak vertical and horizontal circulations. This model will be used as an important tool to investigate the occurrence mechanism of eutrophication and oxygen deficient water masses in Chinhae Bay.

## REFERENCES

Blumberg, A. F. and H. J. Herring, 1987. Circulation modelling using orthonogal curvilinear coordinates, Three-Dimensional Models of Marine and Estuarine Dynamics, J. C. J. Nihoul and B.M. Jamart ed., Elsevier, Amsterdam, The Netherlands: 55-88.

Horiguchi, T., I. Tomita and T. Horie, 1977. On the numerical solutions of three-dimensional hydrodynamic and diffusion. Proc. 24th Confer. of Coastal Eng., JSCE: 443-447.

Kim, C., 1992. Transport mechanism and three-dimensional transport model of cohesive sediment. Ph. D. thesis, National Fisheries University of Pusan, Pusan, Korea, 184 pp.

Kim, C., J. Lee and S. Chang, 1993. Development of three-dimensional baroclinic hydrodynamic model and flow patterns of Suyoung Bay. *J. Oceanol. Soc. Korea*, **28**: 86-100.

Kim, C., S. Chang and J. Lee, 1994. Two-dimensional hydraulic and numerical modeling of tidal currents in Chinhae Bay. *J. Oceanol. Soc. Korea*, **29** (This number).

Kim, J.-H., 1984. Sea water exchange in Chinhae Bay. Ms. thesis, National Fisheries University of Pusan, Pusan, Korea, 39 pp.

KORDI, 1983. A study on the monitoring system for red tides (Jinhae Bay). KORDI Report No. BSPE 00048-80-7, 222 pp.

Large, W.G. and S. Pond, 1981. Open ocean momentum flux measurements in moderate to strong winds. *J. Phys. Oceanogr.*, **11**: 324-336.

Lee, P. Y., J. S. Park, C. M. Kang, H. G. Choi and J. S. Park, 1993. Studies on oxygen-deficient water mass in Chinhae Bay, Bulletin of National Fisheries Research Development and Agency, Report No. 47: 25-38.

Leendertse, J. J. and S. K. Liu, 1975. A three-dimensional model for estuaries and coastal seas: Vol. II, Aspects of computation. R-1764-OWRT, The Rand Corp., 123 pp.

NFRDA, 1989. A comprehensive study on marine pollution for the conservation of the Korean coastal ecosystem with respect to culture areas and fishing grounds. Technical Report No. 84, 347 pp.

Oey, L.-Y., 1988. A model of Gulf Stream frontal instabilities, meanders and eddies along the continental slope. *J. Phys. Oceanogr.*, **18**: 211-229.

Sheng, Y. P., 1983. Mathematical modeling of three-dimensional coastal currents and sediment dispersion: Model development and application. CERC-83-2, US Army Corps of Engineers Waterways Experiment Station, Vicksburg, Miss., Also ARAP Report No. 458, Princeton, NJ, 288 pp.

Yanagi, T., 1980. Variability of the constant flow in Osaka Bay. *J. Oceano. Soc. Japan*, **36**: 246-252

Yanagi, T., K. Azetsu, K. Honda and R. Tatsukawa, 1986. A numerical simulation of suspended sediments flocculation in the estuary. *La mer*, **24**: 202-209.

Accepted April 12, 1994